NASA Technical Memorandum 103251

Numerical Study of Unsteady Shockwave Reflections Using an Upwind TVD Scheme

Andrew T. Hsu
Sverdrup Technology, Inc.
Lewis Research Center Group
Brook Park, Ohio

and

Meng-Sing Liou
National Aeronautics and Space Administration
Lewis Research Center
Cleveland, Ohio

August 1990

NASA

NUMERICAL STUDY OF UNSTEADY SHOCKWAVE REFLECTIONS USING AN UPWIND TVD SCHEME

Andrew T. Hsu
Sverdrup Technology, Inc.
Lewis Research Center Group
Brook Park, Ohio 44142

and

Meng-Sing Liou
National Aeronautics and Space Administration
Lewis Research Center
Cleveland, Ohio 44135

I. Introduction

A three-dimensional, finite volume, time accurate, TVD flow code has been developed recently to solve the full compressible Navier-Stokes equations.[1] This flow solver employs Roe's flux difference splitting for the inviscid fluxes. A unified formulation was introduced for the interpolation of the fluxes on the cell surfaces so that central or upwind schemes of various orders of accuracy can be selected by changing parameters in the formula. A second order predictor corrector scheme is used for the time integration of the equations. In Ref. 1 we have shown that the scheme has very good shock capturing capability.

A moving shock impinging on a circular cylinder produces interesting shock deflection phenomena. As the shock move along the solid surface, shock reflection changes from simple reflection to Mach reflection, causing complicated shock and slip line patterns. These phenomena have been studied both experimentally and numerically.[2,3]

In the present work, the above described computer code is used to study the problem

of moving shocks passing objects. This problem not only requires the scheme to have good shock capturing capability (non-oscillatory) and good time accuracy, but also requires the scheme to be able to treat regions of very low Mach number, for the flowfield in front of the shock has zero Mach number and near the stagnation point in front of the object (e.g. a circular cylinder) the Mach number is very small. Codes that use ADI schemes are known to have difficulties in treating such regions.

The purposes of this paper is to demonstrate the ability of the present numerical scheme to treat such complex unsteady shock reflection problems as well as to provide detailed information on the flow physics of these flowfields. Experimental studies can provide useful information about a flow, but they can not supply with very detailed information. Therefore, the compliment of numerical studies is deemed important.

Numerical Scheme

The full Navier-Stokes equations in conservation law form are used in the present study:

$$\partial_t U + \partial_x E + \partial_y F = Re^{-1}(\partial_x E_v + \partial_y F_v) \tag{1}$$

where U is a vector containing the conservation variables:

$$U = \begin{pmatrix} \rho \\ \rho u \\ \rho v \\ E \end{pmatrix}$$

The vectors E and F are the inviscid flux vectors:

$$E = \begin{pmatrix} \rho u \\ \rho u^2 + p \\ \rho uv \\ u(E+p) \end{pmatrix} \qquad F = \begin{pmatrix} \rho v \\ \rho uv \\ \rho v^2 + p \\ v(E+p) \end{pmatrix}$$

and E_v and F_v are the viscous flux vectors:

$$E_v = \begin{pmatrix} 0 \\ \tau_{xx} \\ \tau_{xy} \\ u\tau_{xx} + v\tau_{xy} - \frac{K}{\beta_r P_r}\frac{\partial T}{\partial x} \end{pmatrix}$$

$$F_v = \begin{pmatrix} 0 \\ \tau_{xy} \\ \tau_{yy} \\ u\tau_{xy} + v\tau_{yy} - \frac{K}{\beta_r P_r}\frac{\partial T}{\partial y} \end{pmatrix}$$

where $\tau_{xx} = (\lambda + 2\mu)u_x + \lambda v_y$, $\tau_{xy} = \mu(u_y + v_x)$, and $\tau_{yy} = (\lambda + 2\mu)v_y + \lambda u_x$.

Define $F_\xi = S_{\xi x}F + S_{\xi y}G$, etc., where $S_{\xi x}$ and $S_{\xi y}$ are components of the surface vector of the numerical cells, then the Navier-Stokes equations can be discretized using a finite volume scheme as

$$(v\frac{dU}{dt})_{i,j} \quad +(F_\xi - F_{v\xi})_{i+\frac{1}{2},j} - (F_\xi - F_{v\xi})_{i-\frac{1}{2},j} \tag{0.2}$$

$$+(F_\eta - F_{v\eta})_{i,j+\frac{1}{2}} - (F_\eta - F_{v\eta})_{i,j-\frac{1}{2}} \tag{0.3}$$

$$= 0, \tag{0.4}$$

where v is the volume of the numerical cell. Thus the equation has been discretized in a general curvilinear coordinate system. The differences between various numerical schemes

are in the ways the fluxes on the numerical cell surfaces are constructed. It is well known that central difference causes odd and even decoupling and the dispersive error thus generated produces oscillations the the solution. While adding artificial viscosity can alleviate this problem, it often causes too much undesired numerical dissipation and hence the decadence of the solution. The TVD schemes developed in recent years are devised to overcome this difficulty by controlling the amount of artificial dissipation in the numerical formulation.

In recent years, upwind schemes are generally preferred in solving hyperbolic equations because of the justifications found in theory of characteristics. In order to apply upwind difference or upwind interpolation, we need to first decompose an inviscid flux into the sum of one flux with only positive eigenvalues and one flux with only negative eigenvalues. In the present work, Roe's flux-difference splitting is employed to decompose the fluxes.

Roe's flux-difference splitting is constructed by relating the flux difference at two arbitrary states, L and R, with the difference of variables U such that

$$\begin{aligned} \Delta F &= \hat{A}\Delta U, \\ \hat{A} &= A(\hat{U}), \quad A(U) = \frac{\partial F}{\partial U}, \\ \hat{U} &= \hat{U}(U_L, U_R). \end{aligned}$$

The object is to find an average state $\hat{U}$ so that the first equation is satisfied exactly for all admissible pairs (U_L, U_R). Since the eigenvalues of the Jacobian matrix A are real, the splitting of these eigenvalues according to their signs leads to the splitting of A:

$$A = A^+ + A^-.$$

The flux difference is split accordingly,

$$\Delta F = \Delta F^+ + \Delta F^- = \hat{A}^+ \Delta U + \hat{A}^- \Delta U.$$

Although the Roe splitting in Cartesian coordinates can be easily constructed, it is less straightforward in general coordinates within the framework of finite-volume discretization, where the geometric metrics are involved. A detailed derivation of the Roe splitting in three-dimensional general curvilinear coordinates was given by the present authors in Ref. 1.

Once the positive and negative flux differences are given, upwind interpolations for the positive and negative fluxes of various orders of accuracy can be constructed as follows. Let

$$F_{i+\frac{1}{2}} = F^+_{i+\frac{1}{2}} + F^-_{i+\frac{1}{2}}$$

where the '+' and '−' components respectively correspond to nonnegative and nonpositive characteristic speeds. Thus upwind polynomial interpolation of fluxes using nodal (cell center) values gives the following formulas for the 'positive' flux:

$$\begin{aligned} F^+_{i+\frac{1}{2}} &= F^+_i + \theta a^+_i \Big\{ \frac{1}{\alpha_i}(1-\kappa)\Delta^- F^+_i + \alpha_i(1+\kappa)\Delta^+ F^+_i & (0.5) \\ &\quad + \sigma\beta_i(\Delta^+ F^+_i - \frac{1}{\alpha_i}\Delta^- F^+_i)\Big\} = F^+_i + \delta^+_i, & (0.6) \end{aligned}$$

and for the 'negative' flux:

$$\begin{aligned} F^-_{i+\frac{1}{2}} &= F^-_{i+1} - \theta a^-_{i+1} \Big\{ \alpha_{i+1}(1-\kappa)\Delta^+ F^-_{i+1} + \frac{1}{\alpha_{i+1}}(1+\kappa)\Delta^- F^-_{i+1} & (0.7) \\ &\quad + \sigma\beta_{i+1}(\Delta^+ F^-_{i+1} - \frac{1}{\alpha_{i+1}}\Delta^- F^-_{i+1})\Big\} = F^-_{i+1} - \delta^-_{i+1}. & (0.8) \end{aligned}$$

where

$\theta = 0$	first-order upwind		
$\theta = 1$	$\sigma = 0$	$\kappa = 1$	second-order central
		$\kappa = -1$	second-order full-upwind
		$\kappa = 0$	Fromm
	$\sigma = 1$	$\kappa = 0$	third-order biased

and let ℓ_i = width of cell i in the ξ-direction;

$$\begin{aligned} \alpha_i &= \frac{\ell_i + \ell_{i-1}}{\ell_i + \ell_{i+1}}; \\ \beta_i &= \frac{\ell_i}{\ell_i + \ell_{i+1}}; \\ a_i^{\pm} &= \frac{\ell_i}{(1 \pm \kappa)(\ell_i + \ell_{i-1}) + (1 \mp \kappa)(\ell_i + \ell_{i+1})}. \end{aligned}$$

The first term in (2.3a) and (2.3b) is identified as the first-order upwind scheme, while the remaining higher-order terms are called the anti-diffusive terms [23]. Combining eqns (2.3a) and (2.3b), we obtain

$$F_{i+\frac{1}{2}} = \frac{1}{2}(F_i + F_{i+1}) - \frac{1}{2}\Delta^+(F_i^+ - F_i^-) + (\delta_i^+ - \delta_{i+1}^-).$$

The first term is a simple-average representation of the interface flux [13], but neglects the nonuniformity of cells. The first two terms together constitute the first-order upwind scheme.

It is a well known fact that first order upwind scheme, although very stable, is too diffusive. On the other hand, the dispersive errors contained in the higher order schemes cause oscillations in the solution. A compromise can be reached by using a limiter to limit the anti-diffusinve terms in eqs. (3) and (4) such that when oscillations occurs, the limiter would turn off the anti-diffusive terms; while for smooth solution, the formulas return to their higher order forms.

The construction of a limited flux is nonlinear and requires modification in the high-order interpolation. This amounts to performing the following modifications in eqs. (3) and (4):

$$\begin{aligned} F^+_{i+\frac{1}{2}} &= F_i^+ + \theta a_i^+ \Big\{ \tfrac{1}{\alpha_i}(1-\kappa)\varphi(r_i^+)\Delta^- F_i^+ \\ &\quad +\alpha_i(1+\kappa)\varphi(\tfrac{1}{r_i^+})\Delta^+ F_i^+ \\ &\quad +\sigma\beta_i[\varphi(\tfrac{1}{r_i^+})\Delta^+ F_i^+ - \tfrac{1}{\alpha_i}\varphi(r_i^+)\Delta^- F_i^+] \Big\}, \end{aligned}$$

$$\begin{aligned} F^-_{i+\frac{1}{2}} &= F^-_{i+1} - \theta a^-_{i+1} \Big\{ \alpha_{i+1}(1-\kappa)\varphi(r^-_{i+1})\Delta^+ F^-_{i+1} \\ &\quad +\tfrac{1}{\alpha_{i+1}}(1+\kappa)\varphi(\tfrac{1}{r^-_{i+1}})\Delta^- F^-_{i+1} + \\ &\quad \sigma\beta_{i+1}[\varphi(r^-_{i+1})\Delta^+ F^-_{i+1} - \tfrac{1}{\alpha_{i+1}}\varphi(\tfrac{1}{r^-_{i+1}})\Delta^- F^-_{i+1}] \Big\}. \end{aligned}$$

The 'limiters' φ^+ and φ^- are functions of some appropriate ratio of neighboring flux differences. For a system of equations, there is no unique way of defining these functions. We have found the following set of definitions quite satisfactory over a wide range of problems [4,6,18]:

$$\begin{aligned} r_i^+ &= \frac{<\Delta^+ F_i^+, \Delta^- F_i^+>}{<\Delta^- F_i^+, \Delta^- F_i^+>} \\ r_i^- &= \frac{<\Delta^+ F_i^-, \Delta^- F_i^->}{<\Delta^+ F_i^-, \Delta^+ F_i^->} \end{aligned}$$

The Roe's superbee limiter is used in the present study:

$$\varphi(r) = max\{0, min(2r,1), min(r,2)\}.$$

Time Evolution. The time integration integration scheme assembles fluxes entering the cell interfaces and updates the conservative variables at the cell center. The requirement

of a monotonic evolution places restrictions on the recombination stage and thus fixes the limiter function. As stated earlier, time accuracy is required in this evolution stage for transient problems. The present method originates from the Taylor series expansion in time, as was done in the Lax-Wendroff scheme. A two-step scheme with second order time accuracy is given here:

$$
\begin{aligned}
(1): \qquad & U^* = U^n + \Delta t \frac{\partial U^n}{\partial t}, \\
(2): \qquad & U^{**} = U^* + \Delta t \frac{\partial U^*}{\partial t}, \\
& U^{n+1} = \tfrac{1}{2}(U^n + U^{**}).
\end{aligned}
$$

The residual $\frac{\partial U}{\partial t}$ vanishes as the solution approaches a steady state. This scheme is similar in form to various types of predictor-corrector schemes. It is also restricted by the usual CFL stability condition. However, unlike the Lax-Wendroff two-step method, both predictor and corrector steps are identical, with no need of defining a midpoint for the corrector step. This reduces the complexity of evaluating the transport terms in the general curvilinear coordinates. The method recovers the one-step Lax-Wendroff scheme even for nonlinear flux functions, thus preserving second-order time accuracy.

Results and Discussion

Recently the problem of a blast wave passing an obstacle has attracted the attention of both experimentalists and numerical analysists. When a shock wave passes a circular cylinder, a serious of shock-solid boundary interaction occurs. The interaction produces an interesting shock reflection pattern. The unsteady nature and the intricate flow pattern made the problem a challenging one on which to test the ability of a shock capturing unsteady

flow solver.

Figure 1 shows an experimental schlieren photograph given by Ref. 2. The experiment shows that when a planar shock wave first impinge on the cylinder, the shock has a regular reflection on the surface. As the reflection point moves towards downstream, it soon become a Mach reflection and the shock split into three, joined by a triple point. A slip surface (density discontinuity) forms at the triple point. After the moving shock has passed the cylinder, there remain a bow shock in front of the cylinder, and vortices are generated behind the cylinder.

In the present work, a traveling shock of incident Mach number 2.81 impinging on a circular cylinder is numerically simulated with the recently developed upwind unsteady flow solver. The air surrounding the cylinder is originally at rest. The shock is released immediately in front of the cylinder at time equal to zero. The grid used is a polar coordinate system, with 100 points in the radial direction and 360 points in the circumferencial direction. The grid has a stretching in the radial direction.

Figure 2 shows the flowfield properties as the shock just hit the cylinder. The density and pressure contours clearly show a regular shock reflection. In front of the cylinder, there exist a region of very high pressure; this can be observed from the pressure distribution on the cylinder surface, as shown in Figure 2c. This initial period produces the maximum load on the cylinder. It is also worth noting that, as shown in the surface pressure distribution, the reflection point (including two shocks) is captured within five grid points by the present numerical scheme.

As the incident shock moved downstream, the shock reflection became a so called

Mach reflection. In another word, the intersection between the incident shock and the bow shock moved away from the solid surface, forming a triple point. A slip surface (density discontinuity) can be observed at this triple point from the density contours shown in Figure 3a as wiggles in the contours. Though the slip surface does not have the sharp feature as observed in the schlieren photo.

As shown in Figure 4, when the two branches of the incident shock collided at the rear of the cylinder, the crossing of the shocks created a local high pressure. A pair of week shocks can also be observed at about 25 degree and 335 degree; these week shocks are presumably caused by the flow over expansion behind the cylinder.

When the incident shock moved further away from the cylinder, an interesting flow pattern is generated. The shocks seem branched out before they reach the solid surface. A pair of vortices appeared behind the cylinder. This flow pattern can be observed from the contours given in Figure 5.

Concluding Remarks

The newly developed upwind unsteady Navier-Stokes solver was used to study the problem of a blast wave interacting with a circular cylinder. The results show that the current solver can capture moving shocks quite well; it keeps the sharp feature of the incident shock as well as the reflected shocks. The slip surface or density can also be captured, although the calculated results do not show the sharp feature as seen on a schlieren photo. In general, one can conclude that moving shock problems can be numerically simulated with fairly good accuracy using an upwind scheme.

References

1. Liou, M.-S. and Hsu, A.T., "A Time-Accurate Finite-Volume High-Resolution Scheme for Three-dimensional Navier-Stokes Equations," Proceedings of AIAA 9th Computational Fluid Dynamics Conference, Buffalo, N.Y., June 13-15, 1989.

2. Bryson, A.E. and Gross, R., "Diffraction of Strong Shocks by Cones, Cylinders, and Spheres," *J. Fluid Mech.*, Vol. 10, 1961, pp. 1-16.

3. Yang, J.Y., Liu, Y. and Lomax, H., "Computation of Shock Wave Reflection by Circular Cylinders," *AIAA Journal*, Vol. 25, No. 5, May 1987.

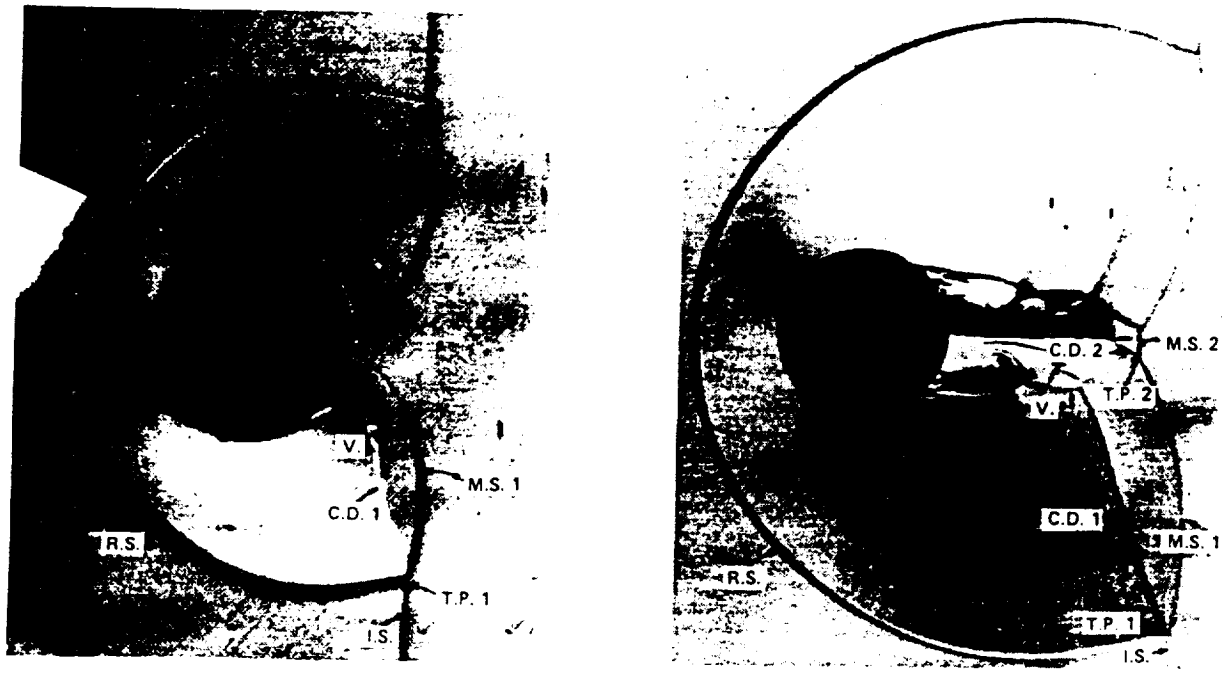

Figure 1. Schlieren photographs of shock wave reflection by a circular cylinder given by Ref. 2.

(Reprinted with the permission of Cambridge University Press, Journal of Fluid Mechanics, Vol. 10, 1961, pp. 1-16, plates 2 and 3, "Diffraction of Strong Shocks by Cones, Cylinders and Spheres" by A. E. Bryson and R. Gross)

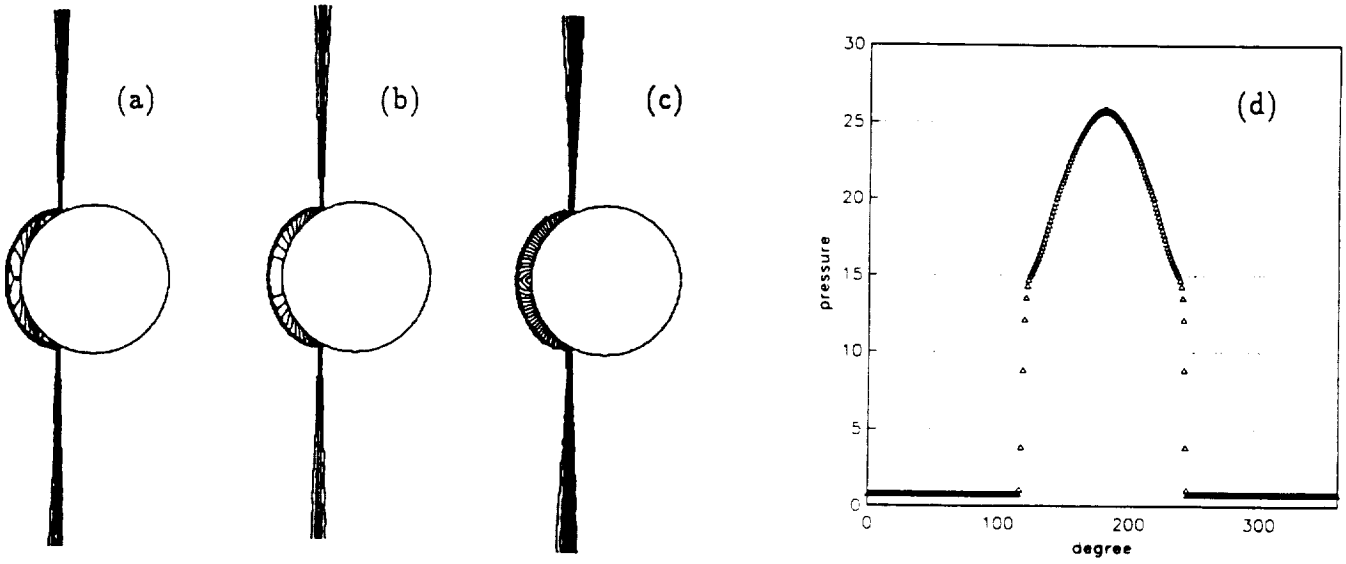

Figure 2. Numerical solution of shock wave reflection: simple reflection; (a) density contours, (b) pressure contours, (c) Mach number contours, (d) wall pressure distribution.

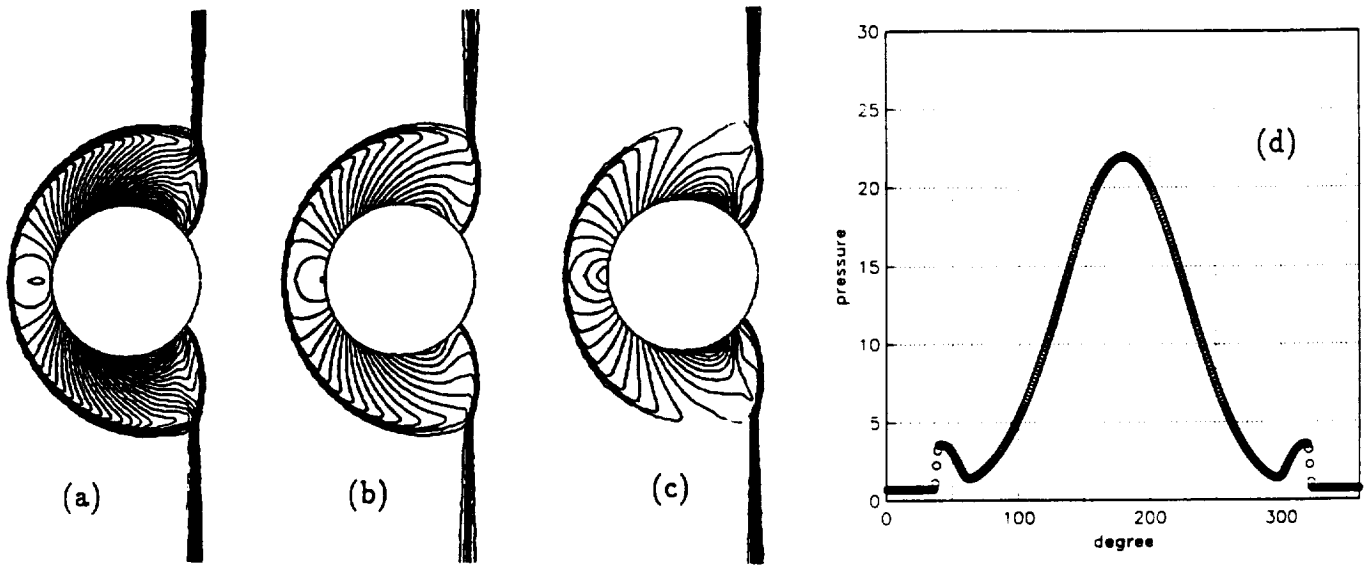

Figure 3. Numerical solution of shock wave reflection: Mach reflection; (a) density contours, (b) pressure contours, (c) Mach number contours, (d) wall pressure distribution.

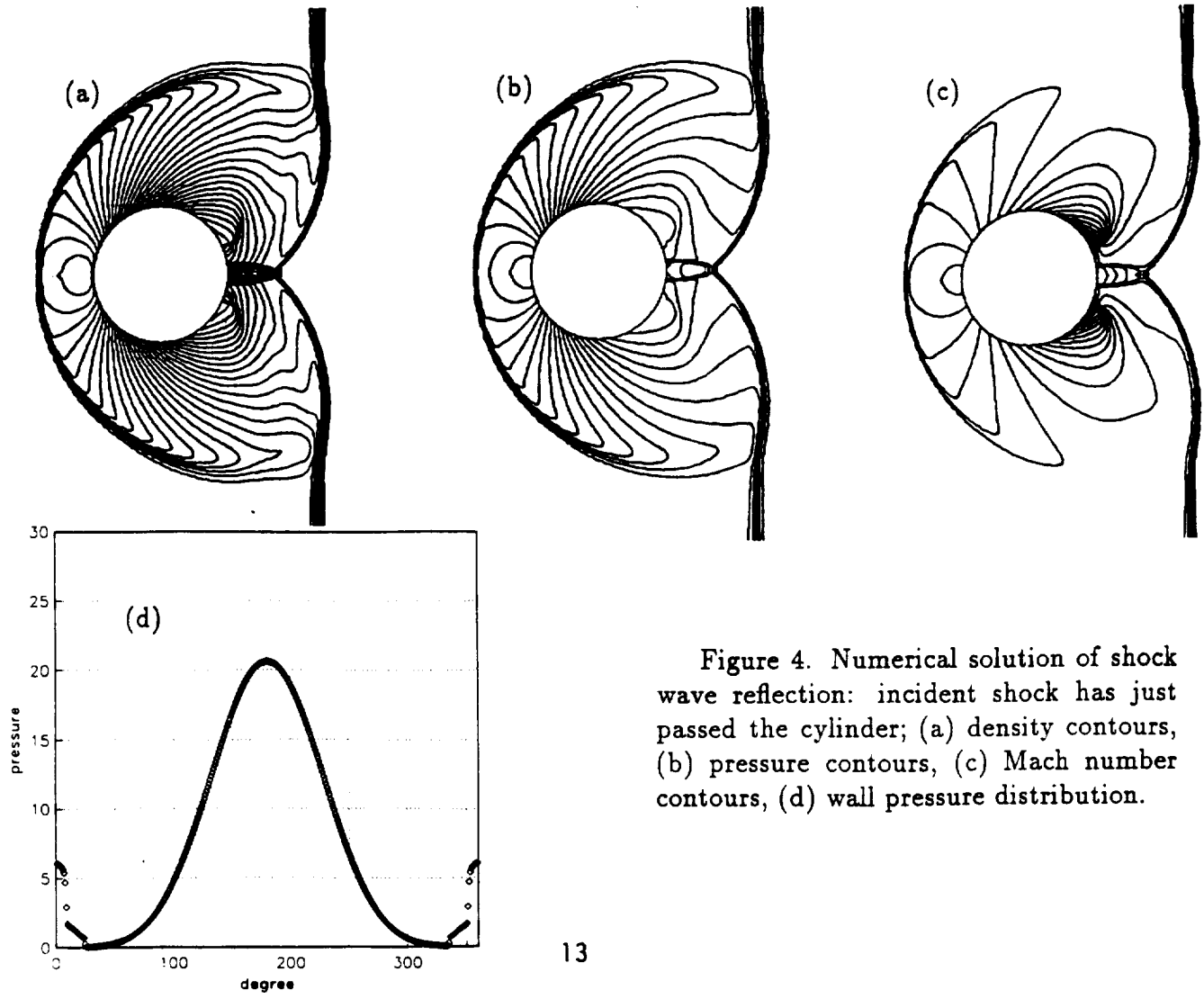

Figure 4. Numerical solution of shock wave reflection: incident shock has just passed the cylinder; (a) density contours, (b) pressure contours, (c) Mach number contours, (d) wall pressure distribution.

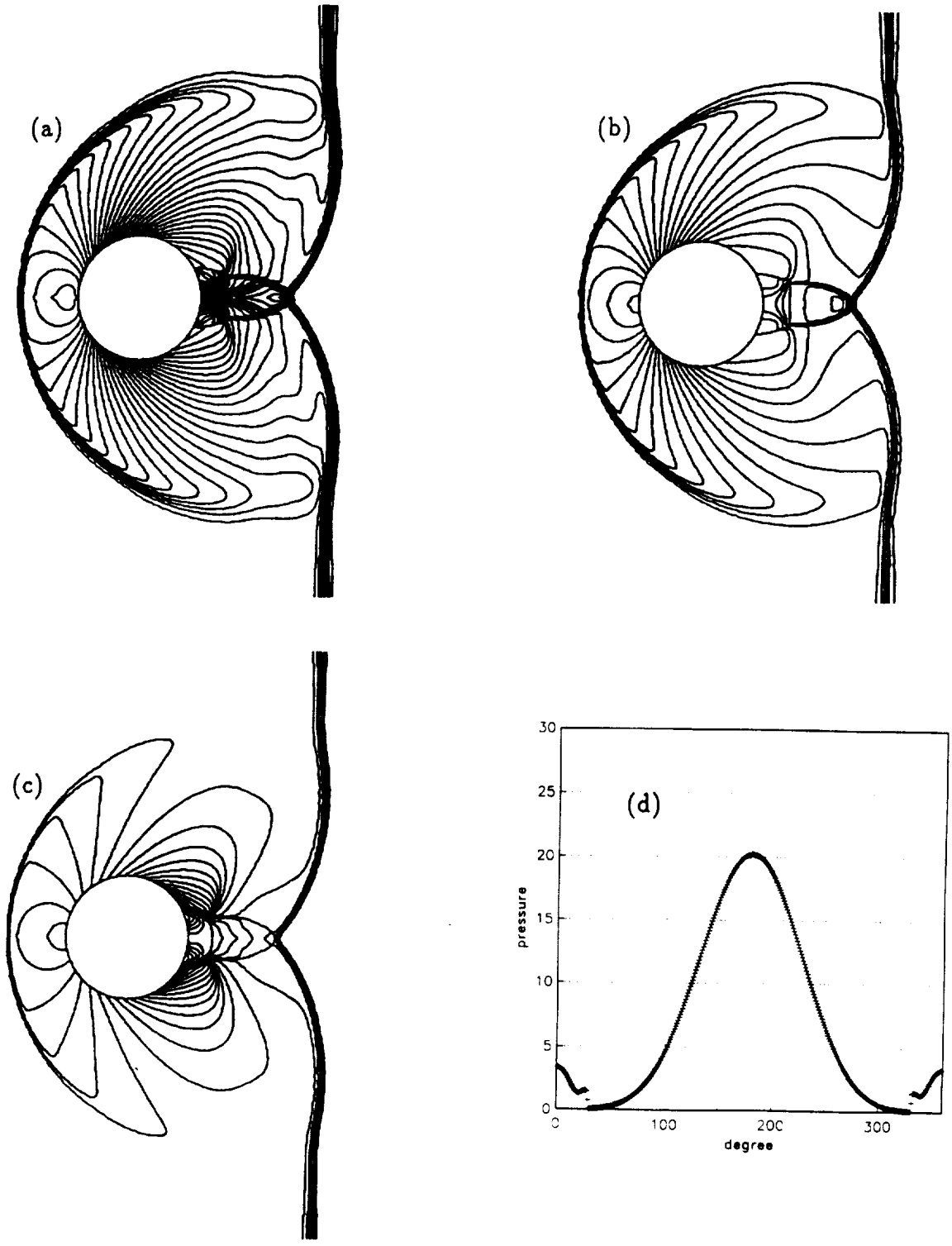

Figure 5. Numerical solution of shock wave reflection: incident shock has moved away from the cylinder; (a) density contours, (b) pressure contours, (c) Mach number contours, (d) wall pressure distribution.

NASA
National Aeronautics and Space Administration

Report Documentation Page

1. Report No.	2. Government Accession No.	3. Recipient's Catalog No.
NASA TM-103251		

4. Title and Subtitle

Numerical Study of Unsteady Shockwave Reflections Using an Upwind TVD Scheme

5. Report Date

August 1990

6. Performing Organization Code

7. Author(s)

Andrew T. Hsu and Meng-Sing Liou

8. Performing Organization Report No.

E-5680

10. Work Unit No.

505-62-21

9. Performing Organization Name and Address

National Aeronautics and Space Administration
Lewis Research Center
Cleveland, Ohio 44135-3191

11. Contract or Grant No.

13. Type of Report and Period Covered

Technical Memorandum

12. Sponsoring Agency Name and Address

National Aeronautics and Space Administration
Washington, D.C. 20546-0001

14. Sponsoring Agency Code

15. Supplementary Notes

Andrew T. Hsu, Sverdrup Technology, Inc., Lewis Research Center Group, 2001 Aerospace Parkway, Brook Park, Ohio 44142; Meng-Sing Liou, NASA Lewis Research Center.

16. Abstract

An unsteady TVD Navier-Stokes solver has been developed and applied to the problem of shock reflection on a circular cylinder. The numerical results obtained from the present study have been compared with the Schlieren photos from an experimental study. These results show that the present computer code has the ability of capturing moving shocks.

17. Key Words (Suggested by Author(s))	18. Distribution Statement
Supersonic Shock reflection CFD	Unclassified – Unlimited Subject Categories 02 and 34

19. Security Classif. (of this report)	20. Security Classif. (of this page)	21. No. of pages	22. Price*
Unclassified	Unclassified	16	A03

*For sale by the National Technical Information Service, Springfield, Virginia 22161